CHAPTER 2

Apolipoprotein B knockdown by AAV-delivered shRNA lowers plasma cholesterol in mice

Annemart Koornneef[1], Piotr Maczuga[1,2], Richard van Logtenstein[1], Florie Borel[1,3], Bas Blits[1], Tita Ritsema[1], Sander van Deventer[2], Harald Petry[1] and Pavlina Konstantinova[1]

[1]Research & Development, Amsterdam Molecular Therapeutics, Amsterdam, the Netherlands; [2]Department of Gastroenterology and Hepatology, Leiden University Medical Center, Leiden, the Netherlands; [3]Department of Gastroenterology and Hepatology, Academic Medical Center, Amsterdam, the Netherlands

Molecular Therapy (2011); 19: *731–740*

Abstract

Serum low-density lipoprotein cholesterol (LDL-C) levels are proportionate to the risk of atherosclerotic cardiovascular disease. In order to reduce serum total cholesterol and LDL-C levels in mice, RNA interference was used to inhibit expression of the structural protein of LDL-C, apolipoprotein B100 (ApoB). We developed and screened 19 short hairpin RNAs targeting conserved sequences in human, mouse, and macaque ApoB mRNAs (shApoB) and subsequently narrowed our focus to one candidate for *in vivo* testing. Self-complementary adeno-associated virus serotype 8 (scAAV8) was used for long-term transduction of murine liver with shApoB. A strong dose-dependent knockdown of ApoB mRNA and protein was observed, which correlated with a reduction in total cholesterol levels, without obvious signs of toxicity. Furthermore, shApoB was found to specifically reduce LDL-C in diet-induced dyslipidemic mice, while high-density lipoprotein cholesterol (HDL-C) remained unaffected. Finally, elevated lipid accumulation was shown in murine liver transduced with shApoB, a known phenotypic side effect of lowering ApoB levels. These results demonstrate a robust dose-dependent knockdown of ApoB by AAV-delivered shRNA in murine liver, thus providing an excellent candidate for development of RNAi-based gene therapy for the treatment of hypercholesterolemia.

Introduction

Elevated levels of serum total cholesterol and low-density lipoprotein cholesterol (LDL-C) are major risk factors and contributors to the development of atherosclerosis and cardiovascular disease (CVD). Currently, hydroxymethylglutaryl coenzyme A reductase inhibitors (statins) are the preferred pharmacologic agents for hypercholesterolemia treatment due to their superior efficacy in lowering LDL-C, proven ability to reduce CVD morbidity and mortality, and a low incidence of adverse events. However, statins are not uniformly effective in all patients and some patients can be relatively refractory to treatment due to absent or diminished LDL-C receptor activity [1]. Furthermore, ten to fifteen percent of patients are unable to take statins due to intolerable muscle symptoms like myalgias, myositis, or mitochondrial injury [2]. Thus, effective therapeutic alternatives with a different mechanism of action are needed.

Apolipoprotein B (ApoB) is required for the assembly of lipoprotein particles and is a constituent of all classes of lipoproteins that are considered atherogenic [3]. ApoB exists in two isoforms, ApoB100 and ApoB48, which are transcribed from a single gene. ApoB100 is the full-length ApoB protein and is synthesized by the liver. It forms the structural protein in very low-density lipoprotein cholesterol (VLDL-C) and LDL-C particles, which are essential for the transport and metabolism of cholesterol. ApoB48 contains the amino-terminal 2152 amino acids of ApoB100 as a result of ApoB mRNA editing which yields an early stop codon. In humans, ApoB is edited solely in the small intestine where ApoB48 plays a role in dietary fat absorption as part of chylomicrons. By contrast, some species such as mice and rats also edit ApoB in their liver and hence synthesize both ApoB100 and ApoB48 [4].

Elevated ApoB levels correlate with increased risk of coronary artery disease [5]. As a large, lipid-associated protein, ApoB belongs to the so-called "non-druggable" targets, which are not amenable to conventional therapies. However, ApoB is a highly validated target for treatment of increased LDL-C levels and subsequent CVD [6]. An approach targeting ApoB with second-generation antisense oligonucleotides (ASO) has progressed into Phase III clinical trials for treatment of homozygous familial hypercholesterolemia [6]. Another therapeutic approach that holds great promise for silencing ApoB is based on RNA interference (RNAi).

RNAi is an evolutionary conserved sequence-specific post-transcriptional gene silencing mechanism in eukaryotes that results in the degradation of mRNA and subsequently in decrease of protein synthesis [7]. Therapeutic RNAi can be induced by synthetic small interfering RNAs (siRNA) or by intracellular expression of short hairpin RNAs (shRNAs) and artificial microRNAs (miRNA) that target a disease-causing gene [8,9,10]. shRNAs are typically expressed from a constitutive strong polymerase III (pol III) promoter, and are processed intracellularly by Dicer, rendering a mature siRNA which interacts with the cytosolic multiprotein RNA-induced silencing complex

(RISC). The RISC-incorporated siRNA binds to the complementary mRNA sequence and mediates its sequence-specific degradation [11].

The largest obstacle in using synthetic siRNAs as therapeutics *in vivo* is the need for efficient and specific delivery to target cells and organs. Chemical modifications and conjugations resulting in lower effective dose and longer half-life of the siRNA have improved their efficacy [12,13]. Chemically modified ApoB-specific siRNAs, when delivered systemically, can silence ApoB expression up to 90% in murine liver [8,14,15]. Inclusion of siApoB in liposomal formulations is another highly effective approach for ApoB silencing in the liver [16]. However, even with current improvements, siRNAs need to be delivered monthly or bi-monthly, which is not achievable for many diseases, especially in the brain, eye, heart, or other internal organs. An alternative for delivery of small RNAs is administration of a single dose of recombinant viral vectors based on lentivirus or adeno-associated virus (AAV), which yield long-term expression [17,18]. The latter holds a unique set of advantages over other vector systems, including the complete lack of pathogenicity and low immunogenicity [19]. AAV induces efficient and long-term transduction of non-dividing cells, an important facet for liver-based gene therapeutic strategies [20]. Unlike the use of synthetic siRNA molecules, AAV gene therapy allows long-term efficacy with a single dose.

In this study, we evaluated the potential of AAV-delivered shRNA for long-term silencing of ApoB in murine liver. A single intravenous injection of AAV-shA10 resulted in prolonged ApoB knockdown with no obvious signs of toxicity, concomitant with a reduction in plasma cholesterol levels. In addition, in mice fed on an atherogenic diet there was a significant reduction of LDL-C, while high density lipoprotein cholesterol (HDL-C) levels remained unchanged.

Results

Design and validation of shRNAs targeting conserved ApoB sequences

Three conserved regions in the last exon of the human, macaque, and mouse ApoB mRNA sequences were selected to design 19 anti-ApoB shRNAs. shApoB expression plasmids (A1-A19) were constructed with the H1 pol III promoter based on a 19-nucleotide target sequence (Table S1). Some of the shRNAs were targeting partly overlapping sequences. For example, shRNAs A9 to A14 were designed by sliding the ApoB target sequence with one nucleotide. All shRNA sequences had identical five-nucleotide loop sequences and the top two basepairs of the pSuper system, and ended with a 3' UU overhang derived from the pol III termination signal.

To evaluate the suppressive activities of the 19 shApoB constructs *in vitro*, we co-transfected them in HEK293T cells with renilla luciferase reporter constructs containing the last ApoB exon in the 3'UTR (Luc-ApoB). An shRNA construct targeting GFP was included as a negative control and firefly luciferase expression was measured

to control for transfection efficiency. Firefly and renilla luciferase expression were measured two days post-transfection and their ratio was used to calculate the relative luciferase activity. The renilla/firefly ratio in the presence of shGFP was set at 100% (Fig. 1a). Four shApoB constructs (A9, A10, A14, and A15) were highly effective and inhibited relative Luc-ApoB expression more than 75%. Ten shApoB constructs (A4, A5, A6, A7, A11, A12, A16, A17, A18, and A19) showed moderate activity and induced 50-75% inhibition of Luc-ApoB. The remaining shApoB constructs were not active. Interestingly, A13 was inactive, whereas the following shRNA construct A14 was highly active, indicating that a single nucleotide shift can render an shRNA ineffective. In total, one out of five tested shApoB constructs was highly active against the Luc-ApoB reporter.

The ability of several shApoB constructs to knockdown endogenous ApoB was assessed *in vitro*. The mouse hepatoma Hepa 1-6 and human hepatoma Huh7 cell lines were transfected with the highly active shApoB constructs A9, A10, A14, and the intermediately active A4, A5, A17, and A18 constructs. As a negative control the shGFP construct was transfected. The three highly active shApoB constructs inhibited murine endogenous ApoB mRNA by approximately 60% while the others were less effective (Fig. 1b). Similar results were obtained for human ApoB knockdown in the Huh7 cell line (data not shown). Generally, the inhibitory effect of the shApoB constructs on endogenous ApoB showed a similar trend to the Luc-ApoB knockdown results.

The highly active shApoB construct A10 (shA10) was selected for further analysis, and siRNA expression from this construct (siA10) was determined *in vitro*. HEK293T cells were transfected with increasing amounts of shA10 plasmid, and two days post-transfection total RNA was isolated and siA10-specific small RNA Taqman assay was performed (Fig. 1c). To calculate the copy number per cell, we used a standard line based on serial dilutions of the guide strand from a synthetic siA10 RNA oligo. Increasing the amount of transfected shA10 construct clearly correlated with an increase in expression of siA10 (Fig. 1c). For example, transfection with 5 ng and 100 ng shA10 construct resulted in approximately 125 and 970 siA10 copies per cell, respectively. Having established a good correlation between shA10 activity and siA10 expression *in vitro*, we proceeded to test the *in vivo* efficacy of this shRNA construct.

Efficient shRNA-mediated knockdown of ApoB and decrease of cholesterol *in vivo*

To test the *in vivo* efficacy of shA10, self-complementary AAV serotype 8 (scAAV8) viral vectors were produced encoding anti-ApoB shA10 or a control shScramble (shScr). C57BL/6 mice were injected via the tail vein with scAAV8-shA10 (AAV-shA10) or the control vector scAAV8-shScramble (AAV-shScr) at four different concentrations: 10^8, 10^9, 10^{10}, and 10^{11} genome copies (gc) per animal. Two weeks after injection, mice

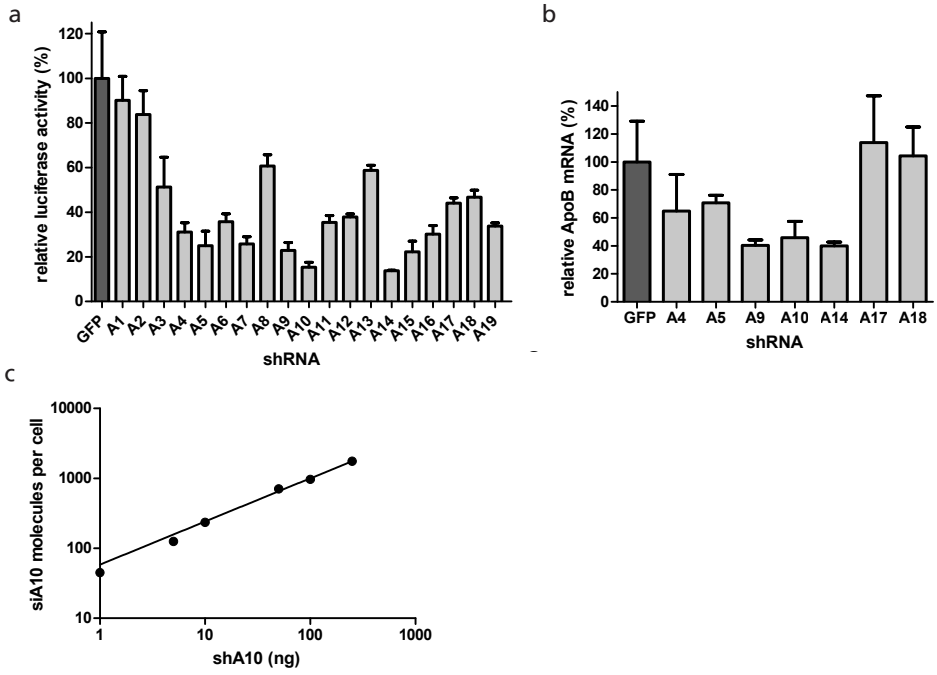

Figure 1. Inhibition of Luc-ApoB reporter and endogenous ApoB mRNA by shApoB constructs *in vitro.* (a) Luc-ApoB knockdown efficiency of anti-ApoB shRNAs expressed from the H1 promoter. HEK293T cells were co-transfected with 10 ng Luc-ApoB reporter and 50 ng different shApoB constructs (A1-A19). The shGFP construct was used as a negative control. Two days post-transfection, firefly and renilla luciferase expression was measured. Renilla luciferase expression was normalized to firefly luciferase expression and shGFP-treated cells were set at 100%. (b) Endogenous ApoB mRNA knockdown by shApoB constructs A4, A5, A9, A10, A14, A17, and A18. The shGFP construct was used as a negative control. Hepa 1-6 cells were transfected with 1 µg shApoB construct. Two days post-transfection, RNA was isolated and qRT-PCR was performed with ApoB- and actin-specific primers. ApoB mRNA levels were calculated relative to actin mRNA and shGFP-treated cells were set at 100%. (c) Small RNA Taqman detection of siA10 expression from shA10. HEK293T cells were transfected with 1, 5, 10, 50, 100, and 250 ng A10 expression construct. Two days post-transfection, RNA was isolated and siA10 Taqman was performed. The transfected amount shA10 correlates well with siA10 expression (R^2=0.997). Data are represented as mean values ±SD from a representative experiment conducted with three technical replicates. Luc, luciferase; ApoB, apolipoprotein B100; shApoB, short hairpin RNA against apolipoprotein B100; shGFP, short hairpin RNA against green fluorescent protein; Hepa 1-6, hepatoma; siA10, small interfering RNA against apolipoprotein B100.

were sacrificed and liver and plasma were analyzed for ApoB knockdown. A dose-dependent increase in AAV transduction efficiency was demonstrated by monitoring GFP fluorescence intensity and GFP mRNA expression in the liver (Figs. 2a and S1), and this correlated with a dose-dependent increase in siA10 and siScr expression (Fig. 2b and data not shown). ApoB mRNA expression in the liver was strongly reduced by administration of increasing doses of AAV-shA10 and reached up to 95% knockdown compared to PBS-injected controls at the highest administered AAV dose

(Fig. 2c). In contrast, the AAV-shScr control vector did not affect ApoB mRNA levels, apart from an unexpected inhibitory effect at the highest dose of 10^{11} gc.

To compare the effect of AAV-shA10 on ApoB mRNA with changes in ApoB protein levels, we assayed plasma and liver ApoB protein levels by Western blot at two weeks post-transduction. AAV-shA10 strongly reduced secreted ApoB100 in a dose-dependent manner, while AAV-shScr did not affect ApoB100 protein expression (Fig. 2d). Similar results were observed for liver ApoB100 protein knockdown (data not shown). In mice, unlike humans, 60-70% of hepatic ApoB mRNA is edited to form truncated ApoB48. Similar to ApoB100, we found that ApoB48 protein levels in plasma and liver were reduced (Fig. 2d and data not shown).These results indicate that a single AAV-shA10 dose achieves a potent knockdown of ApoB mRNA and protein in murine liver and plasma. Furthermore, knockdown of ApoB was associated with changes in total cholesterol levels. Being the structural protein of LDL-C, lowering of ApoB is expected to reduce cholesterol levels. Indeed, dose-dependent ApoB knockdown correlated tightly with reduction in total cholesterol levels, resulting in a maximal cholesterol decrease of 79% compared to PBS-treated controls (Fig. 2e). Profiling of cholesterol distribution over the lipoprotein subclasses revealed a major reduction in HDL-C by AAV-shA10, concomitant with a decrease in VLDL-C and LDL-C levels (Fig. 2f).

AAV-shA10 administration does not cause severe toxicity in mice

It has been reported that high levels of shRNA expression can lead to severe liver toxicity symptoms like weight loss, activation of liver-specific transaminases, changes in liver morphology, or oversaturation of the cellular miRNA machinery [21]. We monitored alanine aminotransferase (ALT) and aspartate aminotransferase (AST) levels two weeks post-transduction with AAV-shA10 and AAV-shScr and observed no significant increase in liver transaminases for the lower viral doses of 10^8, 10^9, and 10^{10} gc per animal. However, the group injected with 10^{11} gc AAV-shScr per animal showed a ten- to thirty-fold increase in ALT and AST levels, indicating liver damage (Fig. 3a). AAV-shA10 injection at a dose of 10^{11} gc per animal gave rise to a two- to five-fold increase in liver transaminases (Fig. 3a). Histological analysis of liver sections revealed no gross changes in liver morphology except for the 10^{11} gc AAV-shScr dose where abnormal morphology was observed (Fig. S2).

shRNAs and miRNAs share the same processing pathway and nuclear export machinery and overexpression of shRNAs can modify the processing of cellular miRNA transcripts [22]. We investigated whether high expression of shRNA in the liver competes with the intracellular processing of miRNAs. mir-122 was selected because it represents 70% of all liver miRNAs and is expressed almost exclusively in the liver [23]. mir-122-specific Taqman analysis was performed on RNA samples isolated from mice two weeks after administration of increasing doses of AAV-shScr

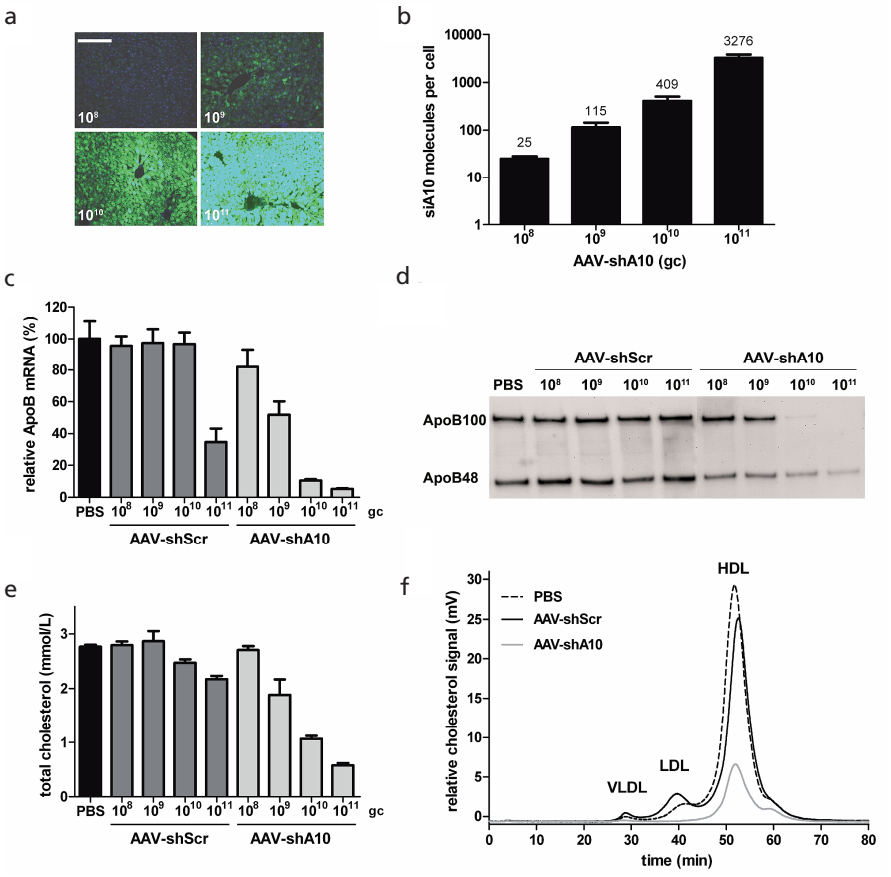

Figure 2. AAV-delivered shA10 strongly inhibits ApoB and plasma cholesterol levels two weeks post-transduction. Mice were intravenously injected with 10^8, 10^9, 10^{10}, and 10^{11} gc AAV-shA10 or control AAV-shScr per animal. Two weeks after transduction, animals were sacrificed and liver and plasma were collected for analysis. (a) Representative image of GFP fluorescence in picric-acid fixed liver, which was transduced with 10^8, 10^9, 10^{10}, or 10^{11} gc AAV-shA10 per animal, co-expressing GFP under control of the liver-specific LP1 promoter. Nuclei were visualized in blue by staining with Hoechst. Photos were taken using the same exposure and magnification settings. Scale bar=10 µm. (b) Small RNA Taqman detection of siA10 expression from liver transduced with 10^8, 10^9, 10^{10}, or 10^{11} gc AAV-shA10 per animal. Total RNA was isolated from snap-frozen livers and siA10-specific Taqman was performed. (c) Relative ApoB mRNA expression in transduced liver. Total RNA was isolated from snap-frozen liver tissue and qRT-PCR was performed with ApoB- and actin-specific primers. ApoB mRNA levels were calculated relative to actin mRNA and the PBS-treated group was set at 100%. (d) Western blot analysis of secreted ApoB100 and ApoB48 protein in 0.1 µL plasma. ApoB protein was detected using a polyclonal anti-ApoB antibody, and antibody binding was visualized by a chemiluminescence detection kit. (e) Total cholesterol levels in plasma collected from fasted mice. Cholesterol levels were analyzed on the automated clinical chemistry analyzer Modular Analytics P800 from Roche. (f) Plasma cholesterol distribution over lipoprotein subclasses in FPLC-separated pooled plasma from mice injected with 10^{11} gc AAV-shA10 or AAV-shScr per animal. Data are represented as mean ±SE, treatment groups are n=5. gc, genome copies; AAV-shA10, adeno-associated virus expressing short hairpin RNA against apolipoprotein B100; AAV-shScr, adeno-associated virus expressing short hairpin RNA scramble; GFP, green fluorescent protein; LP1, liver-specific regulatory element; siA10, small interfering RNA against apolipoprotein B100; FPLC, Fast Protein Liquid Chromatography.

and AAV-shA10. Expression profiles revealed that there was no significant decrease in mir-122 expression except for the group transduced with 10^{11} gc AAV-shScr per animal (Fig. 3b). In this group, mir-122 expression decreased more than 50%. Therefore, we analysed for increased expression levels of AldoA, Bckdk, and Ndrg3, because these genes have been reported as target genes of mir-122 [24]. Gene expression was not significantly affected in murine liver transduced with 10^{11} gc AAV-shScr or AAV-shA10 (Fig. S3). We further monitored the expression of the less abundant liver miRNAs let-7a and mir-29a (Fig. 3b). The expression profile of these miRNAs was similar to mir-122, indicating that there were no severe toxic effects induced by AAV-shA10 or AAV-shScr. Finally, the level of induction of markers of the interferon response (STAT1, TNFα, IFNβ, IFNγ) was examined by qRT-PCR on RNA isolated from murine white blood cells one week after viral administration. No significant induction of the interferon-pathway genes was observed upon viral administration indicating lack of shRNA toxicity at this time-point (data not shown).

ApoB knockdown results in fat accumulation in murine liver

ApoB suppression results in decreased cholesterol levels due to impairment of VLDL-C and LDL-C assembly, but can also lead to hepatic triglyceride accumulation. Triglycerides are normally incorporated into VLDL-C, and hepatic accumulation of these lipids can potentially cause steatosis [14]. To assess the effect of ApoB knockdown on hepatic lipid accumulation, we performed Oil red O staining on liver sections obtained from mice injected with 10^8, 10^9, 10^{10}, or 10^{11} gc AAV-shScr and AAV-shA10 per animal at two weeks post-administration (Fig. 3c). Analysis of the liver sections revealed increased accumulation of hepatic lipid content at the effective 10^9, 10^{10}, and 10^{11} gc AAV-shA10 doses compared with PBS- and AAV-shScr-injected mice (Fig. 3c). In addition, plasma triglyceride levels were also decreased after AAV-shA10 transduction, demonstrating diminished hepatic triglyceride export capacity in these mice (data not shown). These results indicate that a single AAV-shA10 administration in mice results in a dramatically decreased ApoB expression in murine liver with expected phenotypic side effects.

Long-term efficacy of AAV-shA10 in murine liver

In order to monitor the viral persistence and robustness of ApoB knockdown by AAV-shA10, a second group of mice was injected with 10^9 and 10^{11} gc AAV-shA10 or control AAV-shScr and sacrificed at eight weeks post-injection. At this time-point, we observed a significant reduction in ApoB mRNA for both AAV-shA10 viral doses confirming stable transduction of scAAV8 in murine liver (Fig. 4a). However, maximum ApoB mRNA knockdown was slightly less than at two weeks post-transduction (Figs. 2c and 4a). Similarly, GFP and siA10 expression was lower at the eight-week time-point, compared to two weeks post-injection. This effect was most pronounced in the group

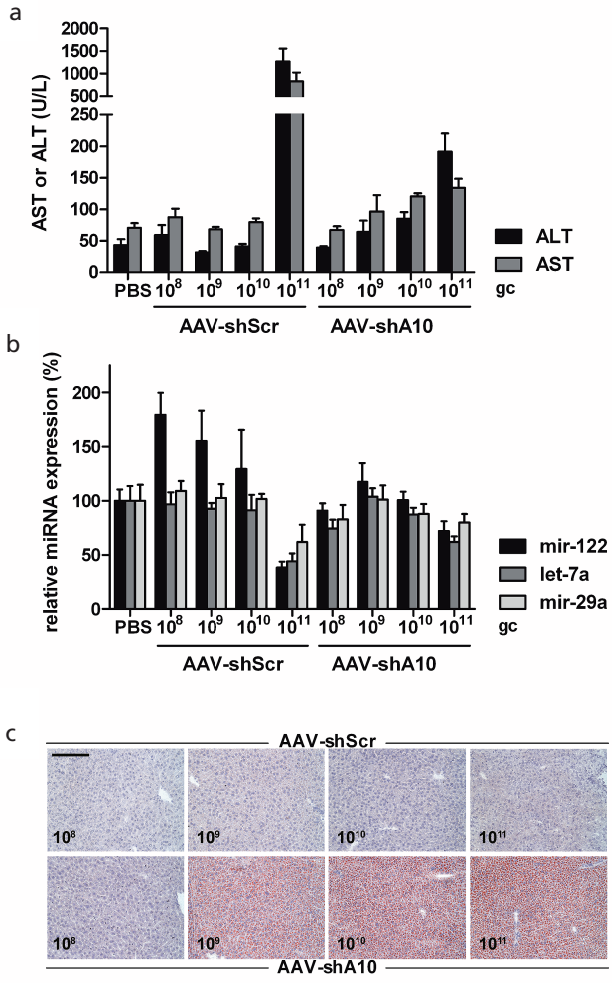

Figure 3. Effect of AAV-delivered shA10 on liver transaminases, cellular miRNA expression, and hepatic fat accumulation. Mice were intravenously injected with 10^8, 10^9, 10^{10}, and 10^{11} gc AAV-shA10 or control AAV-shScr per animal. Two weeks after transduction, animals were sacrificed and liver and plasma were collected for analysis. (a) Liver transaminases ALT and AST at two weeks post-injection. Transaminases were analyzed on the automated clinical chemistry analyzer Modular Analytics P800 from Roche. (b) Relative expression of liver-specific mir-122, let-7a, and mir-29a. Total RNA was isolated from snap-frozen livers and miRNA-specific Taqmans were performed. miRNA expression levels were calculated relative to actin mRNA and the PBS-treated group was set at 100%. Data are represented as mean ±SE, treatment groups are n=5. (c) Representative image of hepatic lipid accumulation. Frozen liver sections were stained with Oil red O for lipids, and nuclei were counterstained with hematoxylin solution. Fat accumulation was visible starting at a dose of 10^9 gc AAV-shA10. Photos were taken using the same exposure and magnification settings. Scale bar=10 µm. gc, genome copies; AAV-shA10, adeno-associated virus expressing short hairpin RNA against apolipoprotein B100; AAV-shScr, adeno-associated virus expressing short hairpin RNA scramble; ALT, alanine aminotransferase; AST, aspartate aminotransferase; mir-122, microRNA 122; let-7a, microRNA let-7a; mir-29a, microRNA 29a; miRNA, microRNA.

of animals injected with the 10^{11} dose (Figs. S4a,b). Nevertheless, AAV-shA10 was still effective at lowering ApoB100 and ApoB48 protein and cholesterol levels (Figs 4b and S4c). AAV-shA10 injection at a dose of 10^{11} gc per animal gave rise to a two- to five-fold increase in liver transaminases, which was most pronounced for ALT levels at three weeks post-injection and transaminases were still above baseline after eight weeks (Fig. 4c). During the eight week period the highest dose of 10^{11} gc AAV-shScr did not induce a dramatic increase in ALT and AST levels, as was observed in the group of animals sacrificed at two weeks post-injection (Figs. 3b and 4c). We next tested for altered expression of mir-122, mir-29a, let-7a, and mir-122 target genes at eight weeks post-injection. No significant changes were measured in liver miRNA or mir-122 target gene expression, although a trend was observed for lower miRNA levels in the animals injected with 10^{11} gc AAV-shA10 (Figs. S4 d,e).

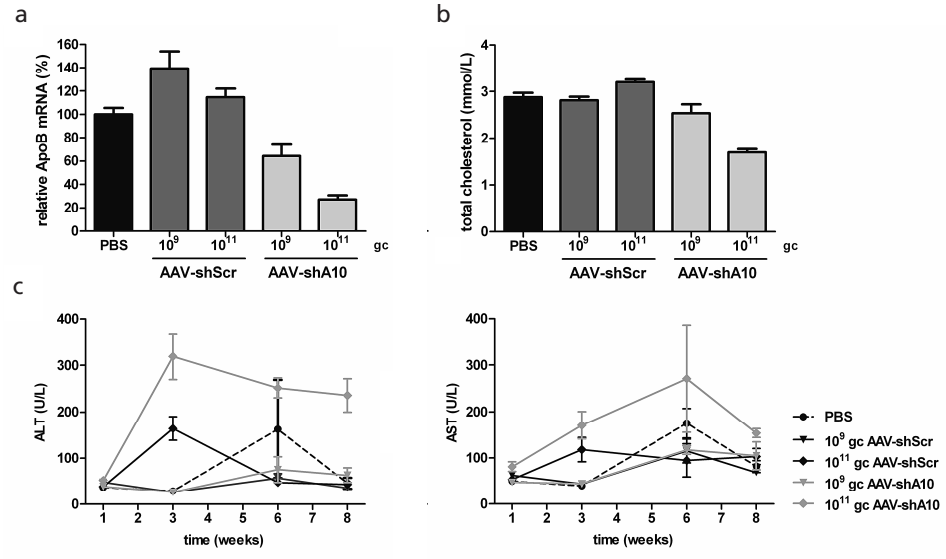

Figure 4. ApoB mRNA and cholesterol decrease eight weeks post-transduction with AAV-shA10. Mice were intravenously injected with 10^9 and 10^{11} gc AAV-shA10 or control AAV-shScr per animal. Eight weeks after transduction, animals were sacrificed and liver and plasma were collected for analysis. (a) Relative ApoB mRNA expression in liver. Total RNA was isolated from snap-frozen liver tissue and qRT-PCR was performed with ApoB- and actin-specific primers. ApoB mRNA levels were calculated relative to actin mRNA and the PBS-treated group was set at 100%. (b) Total cholesterol levels in plasma collected from fasted mice. Cholesterol levels were analyzed on the automated clinical chemistry analyzer Modular Analytics P800 from Roche. (c) Plasma ALT (left panel) and AST (right panel) levels at 1, 3, 6, and 8 weeks post-injection. Transaminases were analyzed on the automated clinical chemistry analyzer Modular Analytics P800 from Roche. Data are represented as mean ±SE, treatment groups are n=5. gc, genome copies; AAV-shA10, adeno-associated virus expressing short hairpin RNA against apolipoprotein B100; AAV-shScr, adeno-associated virus expressing short hairpin RNA scramble; ALT, alanine aminotransferase; AST, aspartate aminotransferase.

AAV-shA10 specifically reduces LDL-C in mice fed on an atherogenic diet

Mice are refractory to atherosclerosis because they have small amounts of VLDL-C and LDL-C, while HDL-C is their major lipoprotein [25]. To specifically elevate VLDL-C and LDL-C levels, mice were fed on an atherogenic diet. Nine weeks after starting on the atherogenic diet, murine livers were grossly enlarged and pale in color, and liver transaminases were elevated compared to lean control animals, as described previously [26] (data not shown). In addition, total cholesterol, VLDL-C, and LDL-C levels increased substantially compared to lean controls (Figs. 2e, 5a-b, S5a). Seven weeks after starting on the atherogenic diet, animals were injected with the effective and non-toxic dose of 10^{10} gc AAV-shA10 or control AAV-shScr per animal, and two weeks later mice were sacrificed and liver and plasma were analyzed for ApoB knockdown. Transduction efficiency in liver cells was lower in atherogenic diet-fed mice compared to lean animals, since GFP mRNA and siA10 expression was respectively hundred- and eight-fold lower (Figs. S5b,c). Nonetheless, AAV-shA10 reduced ApoB mRNA levels by 62% compared to PBS-injected controls, concomitant with a reduction in secreted ApoB100 and ApoB48 protein, whereas AAV-shScr had no effect (Figs. 4d and S5d). Furthermore, ApoB knockdown correlated with a significant reduction in plasma total cholesterol (Fig. 5a). More importantly, AAV-shA10 reduced only VLDL-C and LDL-C levels significantly, while HDL-C concentrations remained unaffected (Figs. 5b-c and S5a).

Discussion

The major challenge for RNAi-based therapies is the delivery of siRNAs to the target tissue or organ. In the last few years much progress has been made in optimizing the specificity and tissue-tropism of AAV viral vectors. AAV vectors mediating expression of shRNAs have proven to be valuable vehicles for RNAi research and therapy of various diseases in the liver, brain, and the eye [9]. However, detailed studies analyzing the dynamics and putative side effects of AAV-shRNA-mediated knockdown of ApoB *in vivo* have not been carried out. To address this issue, we have employed self-complementary AAV serotype 8 that expresses shApoB (AAV-shA10) and have studied prolonged inhibition of ApoB in murine liver. With a single injection of 10^{10} gc per animal of this vector, ApoB expression was inhibited dramatically for up to eight weeks without inducing severe toxicity or disturbance of miRNA processing.

Murine liver was transduced with increasing doses of AAV-shA10 and a good correlation between the administered viral dose and expression of siA10 and GFP mRNA was observed. ApoB knockdown occurred in a dose-dependent fashion and was already detected at a low dose of 10^{9} gc AAV-shA10 per animal, demonstrating the potency of this shRNA construct. Maximal suppression of ApoB led to 95% inhibition of ApoB mRNA and undetectable ApoB100 protein levels, concomitant

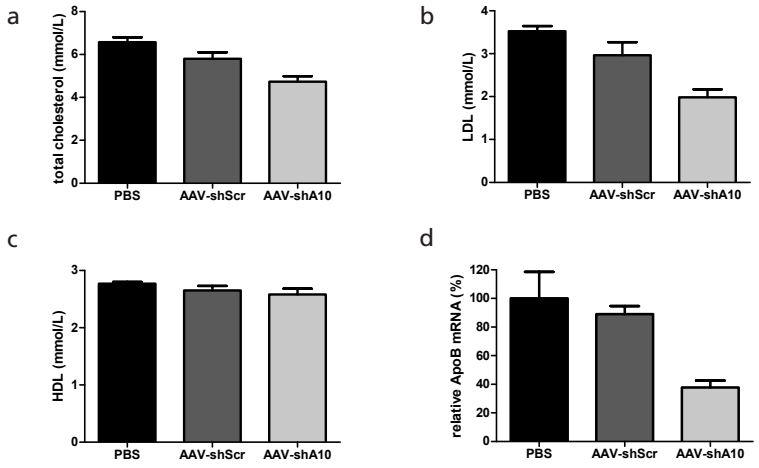

Figure 5. AAV-delivered shA10 specifically lowers total cholesterol and LDL-C levels in mice fed on an atherogenic diet. Mice were fed on an atherogenic diet for seven weeks, before intravenously receiving 10^{10} gc AAV-shA10 or control AAV-shScr per animal. Animals continued feeding on the atherogenic diet and were sacrificed at two weeks post-transduction. (a) Total cholesterol levels in plasma collected from fasted mice. (b) LDL-C levels in plasma collected from fasted mice. LDL-C levels were calculated using the Friedewald formula. AAV-shA10 significantly reduces LDL-C levels compared with PBS (p=0.001) and AAV-shScr (p=0.039) injected animals. (c) HDL-C levels in plasma collected from fasted mice. Cholesterol and HDL-C levels were analyzed on the automated clinical chemistry analyzer Modular Analytics P800 from Roche. (d) Relative ApoB mRNA expression in liver. Total RNA was isolated from snap-frozen liver tissue and qRT-PCR was performed with ApoB- and actin-specific primers. ApoB mRNA levels were calculated relative to actin mRNA and the PBS-treated group was set at 100%. Data are represented as mean ±SE, treatment groups are n=5. gc, genome copies; AAV-shA10, adeno-associated virus expressing short hairpin RNA against apolipoprotein B100; AAV-shScr, adeno-associated virus expressing short hairpin RNA scramble; HDL-C, high-density lipoprotein cholesterol; LDL-C, low-density lipoprotein cholesterol.

with a 79% reduction in plasma total cholesterol. Protein levels of ApoB48 were also reduced by AAV-shA10 in murine plasma and liver. Inhibition of ApoB48 can potentially affect dietary fat absorption in the small intestine. However, AAV-shA10 is not expected to reduce murine intestinal ApoB48, as AAV8 has a manifold higher tropism for liver than intestine [27,28]. Moreover, 85% of intestinal human ApoB transcripts have been shown to terminate after the edited stop codon, which excludes the shA10 target sequence [29]. Hence, AAV-shA10 is not likely to affect the uptake of dietary fats in humans.

We observed a strong reduction in the major lipoprotein in mice, HDL-C, along with a decrease in VLDL-C and LDL-C. The reduction of HDL-C has been attributed to the requirement of components from VLDL-C and LDL-C for the formation of mature HDL-C; hence a significant loss of VLDL-C and LDL-C should result in a similar reduction of HDL-C [30]. There is a debate on to what extent LDL-C levels need to be lowered to achieve optimal cardiovascular risk reduction. It is argued that the

most effective LDL-C intervention is a reduction of at least 30% from baseline, rather than reaching a predefined low LDL-C concentration [31]. Our data show a 32% reduction of plasma total cholesterol after a single intravenous injection with a low dose of 10^9 gc AAV-shA10 per animal, thus signifying potential therapeutic benefit for reducing cardiovascular risk by using this shRNA. To study the specific effect of AAV-shA10 on VLDL-C and LDL-C levels, C57BL/6 mice were fed an atherogenic diet. These mice had elevated levels of plasma total cholesterol, VLDL-C, and LDL-C compared with lean animals. A single administration of 10^{10} gc AAV-shA10 per animal specifically reduced total cholesterol, VLDL-C, and LDL-C levels, while HDL-C remained unaffected, demonstrating the specificity of our approach since ApoB participates only in the formation of VLDL-C and LDL-C, and not HDL-C particles. Similar data have been obtained from human subjects with mild dyslipidemia that were treated with an ApoB ASO [32].

The initial excitement around RNAi as a therapeutic of chronic diseases has been tempered by skepticism related to off-targeting and toxic effects of the shRNA. Recently, it was reported that AAV-expressed shRNAs, when administered to mice, can result in profound liver toxicity, presumably by saturation of the cellular miRNA-processing factors exportin-5 and RISC [21]. shRNA-mediated toxic effects were marked by reductions in cytoplasmic levels of mature miRNA, and were independent of the shRNA sequence. However, toxic effects were due to the injected viral vector dose of 10^{11} and 10^{12} gc per animal, which led to accumulation of extremely high cytoplasmic concentration of the shRNA. The authors discovered that ~10-fold lower viral dose and subsequently lower levels of shRNA expression was effective and well-tolerated, and had no adverse effects [21]. In our study, we were able to achieve a 90% ApoB knockdown at 10^{10} gc AAV-shA10 per animal. At this effective viral dose we did not observe any signs of toxic effects or disturbance of liver mir-122 expression. Similar to the previously published observations of Grimm *et al.* [21], we were able to reach toxic levels of shRNA expression with 10^{11} gc AAV-shScr per animal that was associated with ten to thirty times higher ALT and AST levels, decrease in cellular mir-122 expression, and changes in liver morphology. This strong liver toxicity was probably dependent on the shScr sequence because there was not such a dramatic toxic effect when 10^{11} gc AAV-shA10 per animal was used. The latter induced milder, but persistent ALT and AST activation within the eight-week period, which might be a consequence of the almost complete ApoB inhibition and hepatic fat accumulation at this viral dose. For both AAV-shA10 and AAV-shScr we observed a gradual loss of GFP expression following transduction with the high 10^{11} gc dose, while at 10^9 gc GFP expression persisted more stably within the eight-week study period. These results match previous observations that describe a reduction in transgene expression after transduction with over-expressing shRNAs due to hepatocyte death and subsequent liver repopulation by non-transduced

cells [21,33]. An alternative strategy to avoid shRNA toxicity with no sacrifice in gene-silencing efficacy is to incorporate the siRNA into an artificial miRNA scaffold [34]. It has been suggested that miRNAs are better substrates for Dicer and RISC and therefore get processed more efficiently than shRNAs [10]. Furthermore, they are more amenable to tissue-specific or inducible expression systems than pol III-expressed shRNAs [35]. We are currently testing this hypothesis *in vivo* by incorporating the shA10 sequence in a miRNA backbone (miA10) and correlating the efficacy of miA10 with the concentration of siA10 molecules in mouse livers.

Individuals with the autosomal dominant disorder familial hypobetalipoproteinemia (FHBL) have very low plasma levels of LDL-C and ApoB that are <30% of the normal, and approximately 50% of FHBL subjects carry mutations that result in truncated forms of ApoB. Although these subjects are often clinically asymptomatic, non-alcoholic fatty liver disease (NAFLD) is common due to reduced capacity for hepatic triglyceride export [36,37]. Reduction of ApoB by AAV-shA10 was found to increase the accumulation of hepatic fat content, as determined by Oil red O staining of frozen liver sections, which already occurred at the lowest effective dose of 10^9 gc AAV-shA10 per animal. These results corroborate studies that demonstrated an increase in hepatic lipid content concomitant with ApoB knockdown [14,38,39]. Steatosis was not observed in murine studies with an ApoB ASO [30]. However, treatment of subjects with familial hypercholesterolemia with the human ApoB ASO did reveal a trend toward an increase in intra-hepatic triglyceride content [40]. The clinical relevance of increased hepatic fat content has not been fully elucidated, since follow-up data is lacking on the progression of NAFLD in FHBL patients toward more severe chronic liver diseases, such as steatohepatitis, fibrosis, and cirrhosis [37]. Careful consideration and investigation of this potential consequence of lowering ApoB is warranted. A possible solution to prevent fat accumulation in the liver as a consequence of ApoB knockdown is the use of inducible shRNA expression, for example by the tetracycline inducible (tetO) promoter [41]. Expression of the shApoB can be temporarily "switched on" by addition of doxycycline and when sufficient cholesterol decrease is achieved due to ApoB knockdown, the shRNA expression can be again "switched off". This approach may prevent accumulation of fat in the liver while maintaining the effectiveness of the shApoB in lowering plasma cholesterol levels.

In summary, we showed that ApoB can be almost completely silenced in murine liver by AAV-delivered shRNA. A single injection of 10^{10} gc per animal AAV-shA10 rendered prolonged gene silencing of ApoB that was associated with clear decrease in total plasma cholesterol levels without signs of severe toxicity. Optimization of the shA10 RNA structure by inserting the sequences in a miRNA backbone and obtaining an inducible expression system will be further steps towards a successful gene therapeutic approach for the treatment of hypercholesterolemia.

Matherials and methods

DNA constructs

Nineteen shRNA constructs simultaneously targeting mouse, macaque, and human ApoB, and an shRNA targeting eGFP were made by annealing of complementary oligonucleotides and ligation into the BglII and XhoI site of the pSuper vector (OligoEngine, Seattle, WA). The sequence for constructing the negative control hairpin shScr has been described previously [42]. The sequences of the oligonucleotides used in this study are listed in Table S1. Luciferase reporter Luc-ApoB containing in the 3'UTR 1851 nucleotides of the last exon from human ApoB (NM_000384, 12255-14105) was made by cloning of the ApoB sequence, that was PCR amplified with primers LucApoBf and LucApoBr (Table S1), in the NotI and XhoI sites of the renilla luciferase gene in the psiCHECK-2 vector (Promega, Madison, WI). The Mfold program [43] was used to determine the secondary structure of the RNA transcripts.

For cloning in the AAV backbone, the H1-shRNA expression cassettes were subcloned in pCR-Blunt II-TOPO vector (Invitrogen, Carlsbad, CA), digested with SpeI and XbaI and ligated in the SpeI site of the pVD287 vector. pVD287 contains the eGFP gene under the control of the liver-specific LP1 promoter and generates scAAV due to a mutation in one terminal repeat [44]. Sense orientation of the shRNA cassette was verified by sequencing and the presence of the two ITRs was verified by restriction digestion with SmaI.

Cell culture and transfections

The human embryonic kidney (HEK) 293T, human hepatoma (Huh7), and mouse hepatoma (Hepa1-6) cell lines were maintained in Dulbecco's modified Eagle's medium (DMEM; Invitrogen, Carlsbad, CA) containing 10% fetal calf serum, 100 U/ml penicillin and 100 U/ml streptomycin, at 37°C and 5% CO_2. For luciferase assays, endogenous ApoB knockdown assays, and siRNA expression analysis, cells were seeded in 96- or 24-well plates at a density of 6×10^4 or 1.5×10^5 cells per well, respectively, in DMEM one day prior transfection. Transfections were performed with Lipofectamine 2000 reagent (Invitrogen, Carlsbad, CA) according to the manufacturer's instructions.

Luciferase assays

For luciferase assays, cells were co-transfected with 10 ng Luc-ApoB that contains both firefly and renilla luciferase genes, and 50 ng shApoB expression constructs. Transfected cells were assayed at 48 hr post-transfection in 20 μl 1 x passive lysis buffer (Promega, Madison, WI) by gentle rocking for 15 min at room temperature. The cell lysates were centrifuged for 5 min at 4000 rpm and 10 μl of the supernatant was used to measure firefly and renilla luciferase activities with the Dual-Luciferase Reporter Assay System (Promega, Madison, WI). The relative luciferase activity was calculated as the ratio between the renilla and firefly luciferase activities.

RNA isolation and quantitative real-time RT-PCR

To determine endogenous ApoB mRNA knockdown by the shApoB hairpins *in vitro*, Huh7 and Hepa1-6 cells were transfected with 1 μg shApoB-expressing constructs using Lipofectamine 2000 reagent and total RNA was isolated from cells 48 hr post-transfection using the Nucleospin kit (Clontech, Mountain View, CA). To determine ApoB mRNA knockdown and mir-122 target gene expression *in vivo*, total RNA was isolated from frozen liver sections at two and eight weeks post-transduction with AAV-shA10 using Trizol (Invitrogen, Carlsbad, CA) according to the manufacturer's protocol. Genomic DNA was removed by DNase treatment using TURBO DNase (Ambion, Austin, TX). First strand cDNA was reverse transcribed using random hexamer primers with the Dynamo kit (Finnzymes, Espoo, Finland) and 700 ng of total RNA. Real time PCR amplification was performed with ApoB-, AldoA (Aldolase A)-, Bckdk (Branched-chain α-ketoacid dehydrogenase kinase)-, Ndrg3 (N-myc downstream regulated gene 3)-, and beta actin-specific primers (Table S1). PCR reaction conditions were: 95°C for 10 min, followed by 40 cycles of 15 sec at 95°C and 1 min at 60°C. The assays were performed on ABI 7000 or ABI 7500 (Applied Biosystems, Foster City, CA). ApoB, AldoA, Bckdk, and Ndrg3 expression levels were normalized to beta actin, and the relative gene expression $2^{-\Delta\Delta Ct}$ method of Livak and Schmittgen was used for analysis of PCR data [45].

siRNA and miRNA detection by small RNA Taqman assay

RT reactions for siA10, mir-122, mir-29a, and let-7a expression were performed with the TaqMan MicroRNA Reverse Transcription Kit (Applied Biosystems, Foster City, CA) using 10 ng RNA and 3 μl custom-made specific RT-stem-loop primer (Applied Biosystems, Foster City, CA) according to the manufacturer's instructions. The Taqman assay was done in 20 μl using 1 μl cDNA (15x diluted), 1 μl custom-made siRNA-specific primer with FAM-labelled fluorogenic probe (Applied Biosystems, Foster City, CA) and 10 μl Taqman 2x Universal PCR Master Mix (Applied Biosystems, Foster City, CA). Amplification of the beta actin gene was used as a RNA quality and loading control. siRNA copy number per cell was calculated based on the amplification plot of a dilution series of synthetic siA10 RNA standard (IDT, Coralville, IA). Ten-fold dilutions (100 pg – 1 fg) of the guide strand of a synthetic siA10 RNA oligo were used to create a standard line. The copy number of each dilution was calculated according to the formula 1 mole = 6.02×10^{23} molecules. The trend line value of the standard line was used to calculate the siA10 copy number cell, assuming 15 pg RNA per cell [46]. mir-122, mir-29a, and let-7a expression levels were normalized to beta actin, and the relative gene expression $2^{-\Delta\Delta Ct}$ method of Livak and Schmittgen was used for analysis of PCR data [45].

Western blot analysis for detection of ApoB100 and ApoB48 protein

Murine plasma proteins (0.1 µL) were separated by electrophoresis on a 3-8% Tris-Actetate gel (Invitrogen, Carlsbad, CA) and blotted onto a 0.45 µm nitrocellulose membrane (Invitrogen, Carlsbad, CA). The blot was incubated with a 1:2000 dilution of a rabbit polyclonal anti-ApoB antibody (ab31992, Abcam, Cambrigde, UK), followed by incubation with a 1:2000 dilution of goat anti-rabbit antibody conjugated to horseradish peroxidase (P0448, Dako, Glostrup, Denmark). Antibody binding was detected by the Lumi-Light^{PLUS} chemiluminescent detection kit (Roche Diagnostics, Basel, Switzerland). Equal loading of protein samples was confirmed by Ponceau S staining (Sigma, St. Louis, MO).

AAV vector production

AAV viral vectors were produced encoding shA10 or control shScr and co-expressing the GFP reporter gene under control of the liver-specific LP1 promoter [47]. To maximize efficacy in the murine liver, AAV serotype 8 was employed because it can transduce 100% of hepatocytes in mice when delivered peripherally at high doses [48]. Secondly, a self-complementary AAV (scAAV) vector was used because it shows faster onset of gene expression and 10- to 100-fold higher expression levels than conventional single-stranded vectors [44]. In addition, the scAAV vector is well-suited for expression of short pol III shRNA cassettes, since it cannot accommodate inserts longer than ~2 kb. Self-complementary AAV serotype 8 vectors were produced by calcium phosphate-mediated co-transfection in HEK293T cells, using the three-plasmid based system described by Gao *et al*. [49]. The cells were lysed 48 hr after transfection and virus was released by addition of Tris lysis buffer. Crude lysate from all batches was treated with Benzonase (50 U/mL) (Merck, Darmstadt, Germany) for 1 hr at 37°C. AAV vector particles were purified by iodixanol (Sigma, St. Louis, MO) gradient centrifugation as described previously [50]. Purified batches were concentrated by passage through Vivaspin 15R tubes (Sartorius Stedim, Aubagne, France) to a final concentration of 8-11x10^{11} genome copies (gc) per mL as determined by quantitative PCR with LP1f and LP1r primers amplifying a 95-bp fragment from the LP1 promoter region (Table S1).

In vivo experiments

All animal experiments were conducted according to the guidelines of the local animal welfare committee. Six-to-eight-week-old male C57BL/6 mice received 10^8, 10^9, 10^{10}, or 10^{11} gc AAV-shScr or AAV-shApoB per animal intravenously via the tail vein, corresponding to approximately 4x10^9, 4x10^{10}, 4x10^{11}, or 4x10^{12} gc/kg. Heparinized blood samples were taken at 1, 2, 3, 6, and 8 weeks post-injection from fasted mice for plasma analysis. Mice were sacrificed at two and eight weeks post-injection and livers

and plasma were examined for ApoB knockdown. Feeding was performed *ad libitum* with either regular chow or the atherogenic Paigen diet (TD.88051, Harlan, Madison, WI). Plasma levels of alanine aminotransferase (ALT), aspartate aminotransferase (AST), cholesterol, and high-density lipoprotein cholesterol (HDL-C) were analyzed on the automated clinical chemistry analyzer Modular Analytics P800 (Roche Diagnostics, Basel, Switzerland) at the Academic Medical Center (Amsterdam, the Netherlands). Lipoprotein profiling using FPLC separation of pooled plasma was carried out at the Academic Medical Center (Amsterdam, the Netherlands). GFP expression was analyzed in liver sections that were fixed with 4% formalin, 7% picric acid, and 10% sucrose in PBS. Livers were cryosectioned at 5 µm and eGFP signal was visualized using standard fluorescence microscopy on a Leica fluorescent microscope (Leica Microsystems GmbH, Wetzlar, Germany). Nuclei were visualized by staining with Hoechst. For analysis of liver fat accumulation, snap-frozen liver sections were cryosectioned at 5 µm, fixed in 10% formalin and stained for 25 min in filtered 0.3 % Oil red O (Sigma, St. Louis, MO) solution in 60% isopropanol. Nuclei were counterstained for 5 min in hematoxylin solution (Sigma, St. Louis, MO). Liver histology was assessed by hematoxylin-eosin (H&E) staining of frozen liver sections. Statistical analysis was performed by ANOVA testing and $p<0.05$ was considered significant.

Acknoledgments

The authors thank Han Levels (Academic Medical Center, Amsterdam, the Netherlands) for the FPLC analyses and Eric Timmermans (AMT) and Angelina Huseinovic (AMT) for technical assistance and support. We also thank Jaap Twisk (AMT), Mark Chadwick (AMT), and Wim Hermens (AMT) for critically reviewing the manuscript. The self-complementary AAV vector containing the LP1 promoter was kindly provided by Amit C. Nathwani (St. Jude Children's Research Hospital, Memphis, TN). The authors declare no conflict of interest.

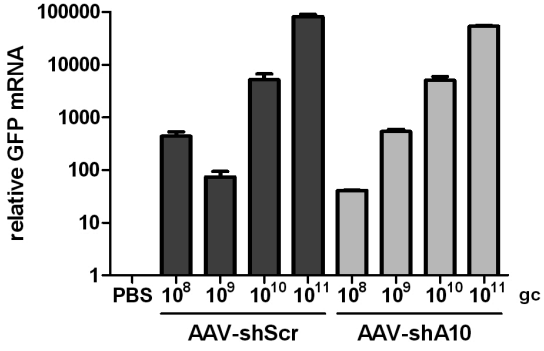

Figure S1. GFP mRNA expression in liver transduced with AAV-shA10 and AAV-shScr. Relative GFP mRNA expression in mice intravenously injected with 10^8, 10^9, 10^{10}, and 10^{11} gc AAV-shA10 or control AAV-shScr per animal. Two weeks post-transduction, RNA was isolated from snap-frozen liver tissue and qRT-PCR was performed with GFP- and actin-specific primers. GFP mRNA levels were calculated relative to actin mRNA and the PBS-treated group was set at 1. Data are represented as mean ±SE, treatment groups are n=5.

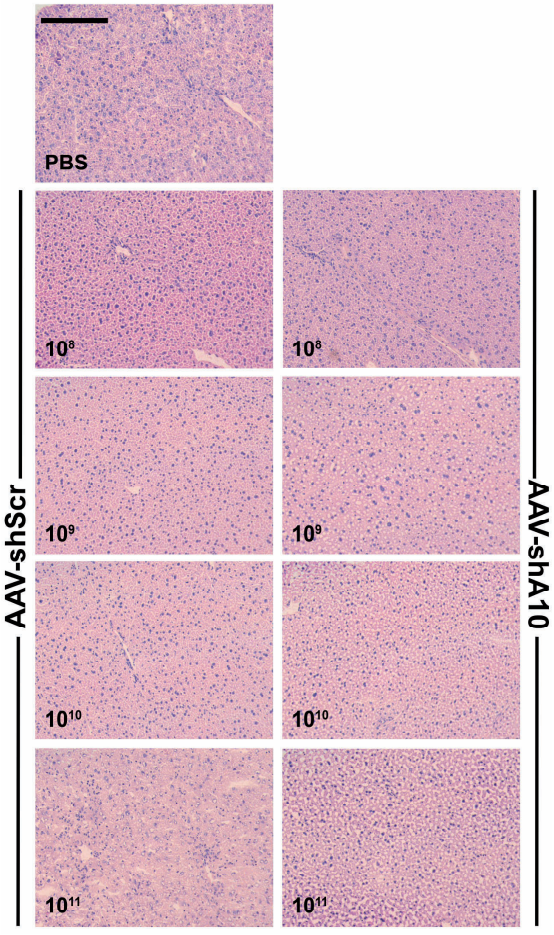

Figure S2. Transduction with 1011 gc AAV-shScr results in abnormal liver tissue morphology, as determined by H&E staining. Representative image of liver sections from mice transduced with 108, 109, 1010, and 1011 gc AAV-shA10 or control AAV-shScr per animal. Animals were sacrificed at two weeks post-transduction and frozen liver tissue was cryosectioned at 5 µm and used for hematoxylin and eosin (H&E) staining. Photos were taken using the same exposure and magnification settings. Scale bar = 10 µm.

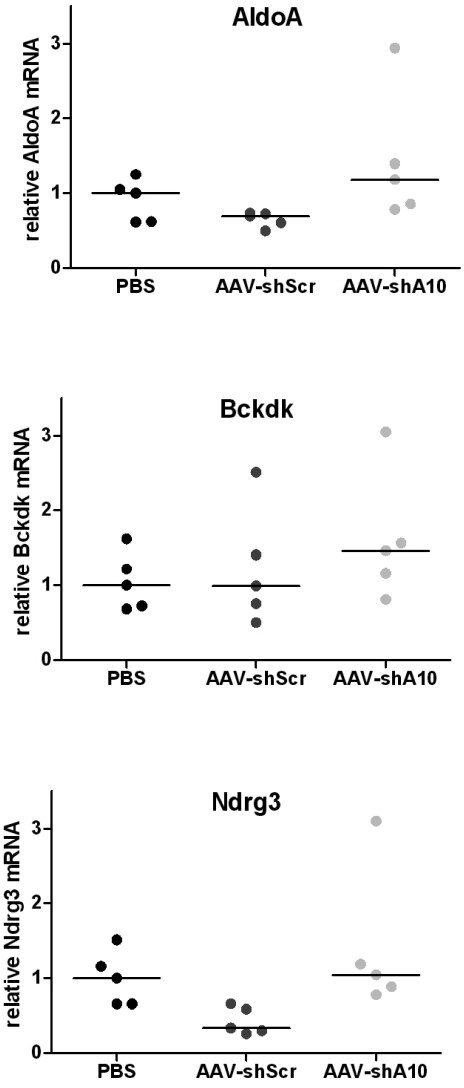

Figure S3. Expression of mir-122 target genes at two weeks post-transduction. Relative expression of mir-122 target genes AldoA, Bckdk, and Ndrg3 in mice transduced with 10^{11} gc AAV-shA10 or control AAV-shScr per animal. Two weeks post-transduction, RNA was isolated from snap-frozen liver tissue and qRT-PCR was performed with AldoA-, Bckdk-, Ndrg3-, and actin-specific primers. AldoA, Bckdk, and Ndrg3 mRNA levels were calculated relative to actin mRNA. Data are represented as individual measurements with median plotted, treatment groups are n=5.

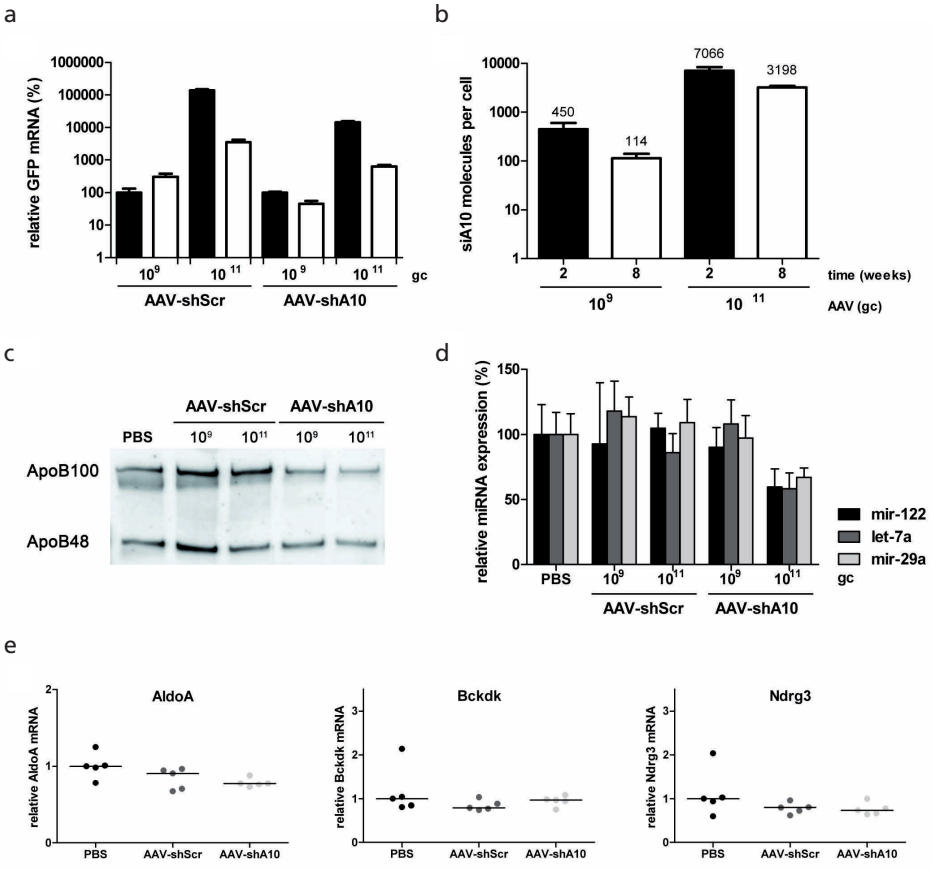

Figure S4. AAV-shA10 persistence, robustness of ApoB knockdown, and off-target effects at eight weeks post-transduction. (a) Comparison of GFP expression in murine liver at two (black bars) and eight (white bars) weeks post-transduction with 10^9 and 10^{11} gc AAV-shA10 or control AAV-shScr per animal. Both viruses co-express the GFP reporter gene under control of a liver-specific LP1 promoter. RNA was isolated from snap-frozen liver tissue, followed by qRT-PCR with GFP- and actin-specific primers. GFP mRNA levels were calculated relative to actin mRNA and the groups injected with 10^9 gc were set at 100%. (b) Comparison of siA10 expression in murine liver at two (black bars) and eight (white bars) weeks post-transduction with 10^9 and 10^{11} gc AAV-shA10 per animal. Total RNA was isolated from snap-frozen livers and siA10-specific small RNA Taqman was performed. The copy number siA10 per cell was calculated as described in Fig. 1c. (c) Western blot analysis of secreted ApoB100 and ApoB48 protein in 0.1 µL plasma eight weeks post-transduction with 10^9 and 10^{11} gc AAV-shA10 or control AAV-shScr per animal. ApoB100 and ApoB48 protein was detected using a polyclonal anti-ApoB antibody, and antibody binding was visualized by a chemiluminescence detection kit. (d) Relative expression of mir-122, let-7a, and mir-29a in murine liver eight weeks post-transduction with 10^9 and 10^{11} gc AAV-shA10 or control AAV-shScr. miRNA-specific Taqmans were performed on RNA isolated from snap-frozen livers, and miRNA expression levels were calculated relative to actin mRNA and the PBS-treated group was set at 100%. Data are represented as mean ±SE, treatment groups are n=5. (e) Relative expression of mir-122 target genes AldoA, Bckdk, and Ndrg3 in mice transduced with 10^{11} gc AAV-shA10 or control AAV-shScr per animal. Eight weeks post-transduction, RNA was isolated from snap-frozen liver tissue and qRT-PCR was performed with AldoA-, Bckdk-, Ndrg3-, and actin-specific primers. AldoA, Bckdk, and Ndrg3 mRNA levels were calculated relative to actin mRNA. Data are represented as individual measurements with median plotted, treatment groups are n=5.

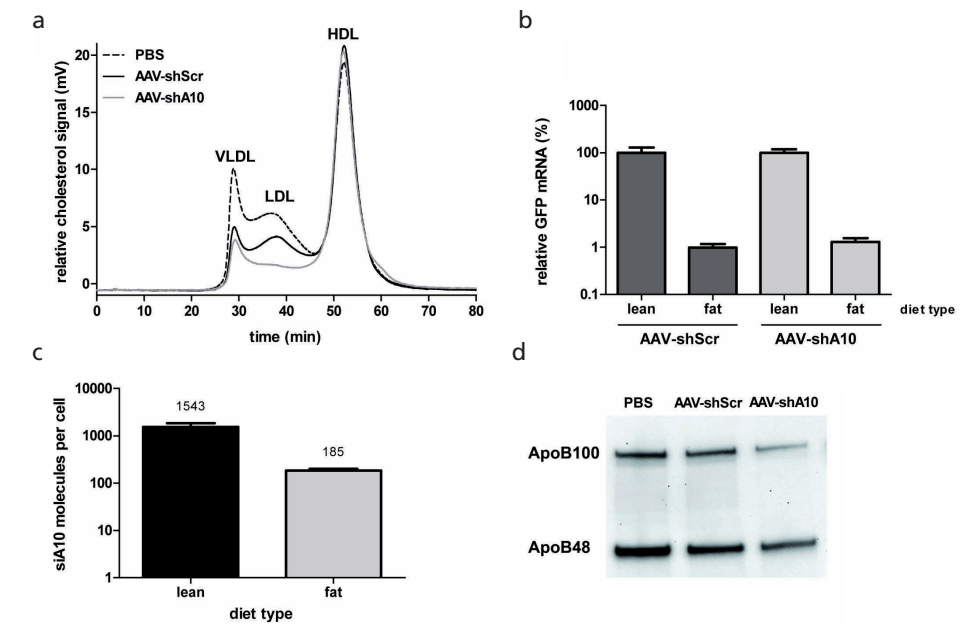

Figure S5. AAV-shA10 persistence and robustness of ApoB knockdown in mice fed on an atherogenic diet. Mice were fed on regular chow (lean) or on an atherogenic diet (fat) containing approximately 15.8% fat, 1.25% cholesterol, and 0.5% sodium cholate for seven weeks, before being injected via the tail vein with 10^{10} gc AAV-shA10 or control AAV-shScr per animal. Animals continued feeding on the atherogenic diet and were sacrificed at two weeks post-transduction. (a) Plasma cholesterol distribution over lipoprotein subclasses in FPLC-separated pooled plasma. (b) Comparison of GFP expression in liver from AAV-transduced mice fed on a regular (lean) or atherogenic (fat) diet. Both AAV-shA10 and AAV-shScr co-express the GFP reporter gene under control of a liver-specific LP1 promoter. Total RNA was isolated from snap-frozen liver tissue and qRT-PCR was performed with GFP- and actin-specific primers. GFP mRNA levels were calculated relative to actin mRNA and the groups of lean mice were set at 100%. (c) Comparison of siA10 expression in liver from AAV-shA10 transduced mice fed on a regular (lean) or atherogenic (fat) diet. Total RNA was isolated from snap-frozen livers and siA10-specific small RNA Taqman assay was performed. The copy number siA10 per cell was calculated as described in Fig. 1c. (d) Western blot analysis of secreted ApoB100 and ApoB48 protein in 0.1 µL plasma from mice that were fed on an atherogenic diet and transduced with 10^{10} gc AAV-shA10 or control AAV-shScr. ApoB100 and ApoB48 protein was detected using a polyclonal anti-ApoB antibody, and antibody binding was visualized by a chemiluminescence detection kit. Data are represented as mean ±SE, treatment groups are n=5.

Table S1. Oligonucleotides used in this study

name	Sequence (5′-3′)	Target
shA1f	GATCCCC**TTAATTGGGAAGAAGAGGC**TTCAAGAGA**GCCTCTTCTTCCCAATTAA**TTTTTC	ApoB, 12295-12313
shA1r	TCGAGAAAAATTAATTGGGAAGAAGAGGCTCTCTTGAAGCCTCTTCTTCCCAATTAAGGG	
shA2f	GATCCCC**TAATTGGGAAGAAGAGGCA**TTCAAGAGA**TGCCTCTTCTTCCCAATTA**TTTTTC	ApoB, 12296-12314
shA2r	TCGAGAAAAATAATTGGGAAGAAGAGGCATCTCTTGAATGCCTCTTCTTCCCAATTAGGG	
shA3f	GATCCCC**TTGGGAAGAAGAGGCAGCT**TTCAAGAGA**AGCTGCCTCTTCTTCCCAA**TTTTTC	ApoB, 12299-12317
shA3r	TCGAGAAAAATTGGGAAGAAGAGGCAGCTTCTCTTGAAAGCTGCCTCTTCTTCCCAAGGG	
shA4f	GATCCCC**TGGGAAGAAGAGGCAGCTT**TTCAAGAGA**AAGCTGCCTCTTCTTCCCA**TTTTTC	ApoB, 12300-12318
shA4r	TCGAGAAAAATGGGAAGAAGAGGCAGCTTTCTCTTGAAAAGCTGCCTCTTCTTCCCAGGG	
shA5f	GATCCCC**GGGAAGAAGAGGCAGCTTC**TTCAAGAGA**GAAGCTGCCTCTTCTTCCC**TTTTTC	ApoB, 12301-12319
shA5r	TCGAGAAAAAGGGAAGAAGAGGCAGCTTCTCTCTTGAAGAAGCTGCCTCTTCTTCCCGGG	
shA6f	GATCCCC**TGGACAGTGAAATATTATG**TTCAAGAGA**CATAATATTTCACTGTCCA**TTTTTC	ApoB, 13314-13332
shA6r	TCGAGAAAAATGGACAGTGAAATATTATGTCTCTTGAACATAATATTTCACTGTCCAGGG	
shA7f	GATCCCC**GGACAGTGAAATATTATGA**TTCAAGAGA**TCATAATATTTCACTGTCC**TTTTTC	ApoB, 13315-13333
shA7r	TCGAGAAAAAGGACAGTGAAATATTATGATCTCTTGAATCATAATATTTCACTGTCCGGG	
shA8f	GATCCCC**GACAGTGAAATATTATGAA**TTCAAGAGA**TTCATAATATTTCACTGTC**TTTTTC	ApoB, 13316-13334
shA8r	TCGAGAAAAAGACAGTGAAATATTATGAATCTCTTGAATTCATAATATTTCACTGTCGGG	
shA9f	GATCCCC**AGATTGATTGACCTGTCCA**TTCAAGAGA**TGGACAGGTCAATCAATCT**TTTTTC	ApoB, 13683-13701
shA9r	TCGAGAAAAAAGATTGATTGACCTGTCCATCTCTTGAATGGACAGGTCAATCAATCTGGG	
shA10f	GATCCCC**GATTGATTGACCTGTCCAT**TTCAAGAGA**ATGGACAGGTCAATCAATC**TTTTTC	ApoB, 13684-13702
shA10r	TCGAGAAAAAGATTGATTGACCTGTCCATTCTCTTGAAATGGACAGGTCAATCAATCGGG	
shA11f	GATCCCC**ATTGATTGACCTGTCCATT**TTCAAGAGA**AATGGACAGGTCAATCAAT**TTTTTC	ApoB, 13685-13703
shA11r	TCGAGAAAAAATTGATTGACCTGTCCATTTCTCTTGAAAATGGACAGGTCAATCAATGGG	
shA12f	GATCCCC**TTGATTGACCTGTCCATTC**TTCAAGAGA**GAATGGACAGGTCAATCAA**TTTTTC	ApoB, 13686-13704
shA12r	TCGAGAAAAATTGATTGACCTGTCCATTCTCTCTTGAAGAATGGACAGGTCAATCAAGGG	
shA13f	GATCCCC**TGATTGACCTGTCCATTCA**TTCAAGAGA**TGAATGGACAGGTCAATCA**TTTTTC	ApoB, 13687-13705
shA13r	TCGAGAAAAATGATTGACCTGTCCATTCATCTCTTGAATGAATGGACAGGTCAATCAGGG	
shA14f	GATCCCC**GATTGACCTGTCCATTCAA**TTCAAGAGA**TTGAATGGACAGGTCAATC**TTTTTC	ApoB, 13688-13706
shA14r	TCGAGAAAAAGATTGACCTGTCCATTCAATCTCTTGAATTGAATGGACAGGTCAATCGGG	
shA15f	GATCCCC**TGACCTGTCCATTCAAAAC**TTCAAGAGA**GTTTTGAATGGACAGGTCA**TTTTTC	ApoB, 13691-13709
shA15r	TCGAGAAAAATGACCTGTCCATTCAAAACTCTCTTGAAGTTTTGAATGGACAGGTCAGGG	

shA16f	GATCCCC**GACCTGTCCATTCAAAACT**TTCAAGAGA**AGTTTTGAATGGACAGGTC**TTTTTC	ApoB,13692-13710
shA16r	TCGAGAAAAAGACCTGTCCATTCAAAACTTCTCTTGAAAGTTTTGAATGGACAGGTCGGG	
shA17f	GATCCCC**CCTGTCCATTCAAAACTAC**TTCAAGAGA**GTAGTTTTGAATGGACAGG**TTTTTC	ApoB,13694-13712
shA17r	TCGAGAAAAACCTGTCCATTCAAAACTACTCTCTTGAAGTAGTTTTGAATGGACAGGGGG	
shA18f	GATCCCC**CTGTCCATTCAAAACTACC**TTCAAGAGA**GGTAGTTTTGAATGGACAG**TTTTTC	ApoB,13695-13713
shA18r	TCGAGAAAAACTGTCCATTCAAAACTACCTCTCTTGAAGGTAGTTTTGAATGGACAGGGG	
shA19f	GATCCCC**GTCCATTCAAAACTACCAC**TTCAAGAGA**GTGGTAGTTTTGAATGGAC**TTTTTC	ApoB,13697-13715
shA19r	TCGAGAAAAAGTCCATTCAAAACTACCACTCTCTTGAAGTGGTAGTTTTGAATGGACGGG	
shScr-f	GATCCCCGATCGAATGTGTACTTCGATTCCAAGAGATCGAAGTACACATTCGATCTTTTTGCATGCC	Doege *et al*., 2008
shScr-r	TCGAGGCATGCAAAAAGATCGAATGTGTACTTCGATCTCTTGGAATCGAAGTACACATTCGATCGGG	
shGFPf	GATCCCC**AGCTGGAGTACAACTACAAC**CTTCCTGTCA**GTTGTAGTTGTACTCCAGCT**TTTTGCATGCC	eGFP
shGFPr	TCGAGGCATGCAAAAAGCTGGAGTACAACTACAACTGACAGGAAGGTTGTAGTTGTACTCCAGCTGGG	
LucApoBf	CGACTCGAGTTGAGGGTCCGGGAAT	ApoB,12255-12271
LucApoBr	CGAGCGGCCGCGACTCCATTTATTTGTTCCTCCTC	ApoB,14105-14081
ApoBf	TGGTTACTGCGCTGAGAGG	ApoB qRT-PCR
ApoBr	CCACACTGAACCAAGGCTT	
m-act-f	ACGGCCAGGTCATCACTATTG	Mouse actin qRT-PCR
m-act-r	CAAGAAGGAAGGCTGGAAAAGA	
h-act-f	CAGCCATGTACGTTGCTATCCAGG	Human actin qRT-PCR
h-act-r	AGGTCCAGACGCAGGATGGCATG	
LP1f	CCCTGTTTGCTCCTCCGATAA	LP1 qRT-PCR
LP1r	GTCCGTATTTAAGCAGTGGATCCA	
eGFPf	GGGCACAAGCTGGAGTACAACTA	eGFP qRT-PCR
eGFPr	ATGTTGTGGCGGATCTTGAAG	
AldoA-f	GCTGTGCCCAGTATAAGAAG	AldoA qRT-PCR
AldoA-r	GCTCCACAATGGGTACAATG	
Bckdk-f	TGCTGGCTACTCACCACTTG	Bckdk qRT-PCR
Bckdk-r	ATGTCCGTTGATGCGGACTC	

ApoB (NM_000384) and GFP sequences in the shRNA oligos are bold
Accession numbers of the genes are: mmu-AldoA NM_001177307, mmu-Bckdk NM_009739, mmuNdrg3 NM_013865

Reference list

1. Rader, DJ, Cohen, J and Hobbs, HH (2003). Monogenic hypercholesterolemia: new insights in pathogenesis and treatment. *J Clin Invest*; **111:** 1795-1803.
2. Kashani, A, Phillips, CO, Foody, JM, Wang, Y, Mangalmurti, S, Ko, DT, et al. (2006). Risks associated with statin therapy: a systematic overview of randomized clinical trials. *Circulation*; **114:** 2788-2797.
3. Young, SG (1990). Recent progress in understanding apolipoprotein B. *Circulation*; **82:** 1574-1594.
4. Greeve, J, Altkemper, I, Dieterich, JH, Greten, H and Windler, E (1993). Apolipoprotein B mRNA editing in 12 different mammalian species: hepatic expression is reflected in low concentrations of apoB-containing plasma lipoproteins. *J Lipid Res*; **34:** 1367-1383.
5. Zambon, A, Brown, BG, Deeb, SS and Brunzell, JD (2006). Genetics of apolipoprotein B and apolipoprotein AI and premature coronary artery disease. *J Intern Med*; **259:** 473-480.
6. Raal, FJ, Santos, RD, Blom, DJ, Marais, AD, Charng, MJ, Cromwell, WC, et al. (2010). Mipomersen, an apolipoprotein B synthesis inhibitor, for lowering of LDL cholesterol concentrations in patients with homozygous familial hypercholesterolaemia: a randomised, double-blind, placebo-controlled trial. *Lancet*; **375:** 998-1006.
7. Fire, A, Xu, S, Montgomery, MK, Kostas, SA, Driver, SE and Mello, CC (1998). Potent and specific genetic interference by double-stranded RNA in Caenorhabditis elegans. *Nature*; **391:** 806-811.
8. Soutschek, J, Akinc, A, Bramlage, B, Charisse, K, Constien, R, Donoghue, M, et al. (2004). Therapeutic silencing of an endogenous gene by systemic administration of modified siRNAs. *Nature*; **432:** 173-178.
9. Grimm, D (2009). Small silencing RNAs: State-of-the-art. *Adv Drug Deliv Rev*; **61:** 672-703.
10. Liu, YP, Haasnoot, J, ter Brake, O, Berkhout, B and Konstantinova, P (2008). Inhibition of HIV-1 by multiple siRNAs expressed from a single microRNA polycistron. *Nucleic Acids Res*; **36:** 2811-2824.
11. Zamore, PD, Tuschl, T, Sharp, PA and Bartel, DP (2000). RNAi: Double-stranded RNA directs the ATP-dependent cleavage of mRNA at 21 to 23 nucleotide intervals. *Cell*; **101:** 25-33.
12. Love, KT, Mahon, KP, Levins, CG, Whitehead, KA, Querbes, W, Dorkin, JR, et al. (2010). Lipid-like materials for low-dose, in vivo gene silencing. *Proc Natl Acad Sci U S A*; **107:** 1864-1869.
13. Semple, SC, Akinc, A, Chen, J, Sandhu, AP, Mui, BL, Cho, CK, et al. (2010). Rational design of cationic lipids for siRNA delivery. *Nat Biotech*; **28:** 172-176.
14. Rozema, DB, Lewis, DL, Wakefield, DH, Wong, SC, Klein, JJ, Roesch, PL, et al. (2007). Dynamic PolyConjugates for targeted in vivo delivery of siRNA to hepatocytes. *Proc Natl Acad Sci U S A*; **104:** 12982-12987.
15. Wolfrum, C, Shi, S, Jayaprakash, KN, Jayaraman, M, Wang, G, Pandey, RK, et al. (2007). Mechanisms and optimization of in vivo delivery of lipophilic siRNAs. *Nat Biotech*; **25:** 1149-1157.
16. Zimmermann, TS, Lee, ACH, Akinc, A, Bramlage, B, Bumcrot, D, Fedoruk, MN, et al. (2006). RNAi-mediated gene silencing in non-human primates. *Nature*; **441:** 111-114.
17. Manjunath, N, Wu, H, Subramanya, S and Shankar, P (2009). Lentiviral delivery of short hairpin RNAs. *Adv Drug Deliv Rev*; **61:** 732-745.
18. Grimm, D, Pandey, K and Kay, MA (2005). Adeno-associated virus vectors for short hairpin RNA expression. *Methods Enzymol*; **392:** 381-405.
19. Daya, S and Berns, KI (2008). Gene therapy using adeno-associated virus vectors. *Clin Microbiol Rev*; **21:** 583-593.
20. Vaessen, SF, Veldman, RJ, Comijn, EM, Snapper, J, Sierts, JA, van den Oever, K, et al. (2009). AAV gene therapy as a means to increase apolipoprotein (Apo) A-I and high-density lipoprotein-cholesterol levels: correction of murine ApoA-I deficiency. *J Gene Med*; **11:** 697-707.
21. Grimm, D, Streetz, KL, Jopling, CL, Storm, TA, Pandey, K, Davis, CR, et al. (2006). Fatality in mice due to oversaturation of cellular microRNA/short hairpin RNA pathways. *Nature*; **441:** 537-541.
22. Kim, VN (2005). Small RNAs: Classification, biogenesis, and function. *Mol Cells*; **19:** 1-15.
23. Lagos-Quintana, M, Rauhut, R, Yalcin, A, Meyer, J, Lendeckel, W and Tuschl, T (2002). Identification of tissue-specific microRNAs from mouse. *Curr Biol*; **12:** 735-739.
24. Elmen, J, Lindow, M, Silahtaroglu, A, Bak, M, Christensen, M, Lind-Thomsen, A, et al. (2007). Antagonism of microRNA-122

in mice by systemically administered LNA-antimiR leads to up-regulation of a large set of predicted target mRNAs in the liver. *Nucleic Acid Res*; **36:** 1153-1162.

25. Jiao, S, Cole, TG, Kitchens, RT, Pfleger, B and Schonfeld, G (1990). Genetic heterogeneity of lipoproteins in inbred strains of mice: analysis by gel-permeation chromatography. *Metabolism*; **39:** 155-160.
26. Matsuzawa, N, Takamura, T, Kurita, S, Misu, H, Ota, T, Ando, H, et al. (2007). Lipid-induced oxidative stress causes steatohepatitis in mice fed an atherogenic diet. *Hepatology*; **46:** 1392-1403.
27. Nakai, H, Fuess, S, Storm, TA, Muramatsu, Si, Nara, Y and Kay, MA (2005). Unrestricted hepatocyte transduction with adeno-associated virus serotype 8 vectors in mice. *J Virol*; **79:** 214-224.
28. Shen, X, Storm, T and Kay, MA (2007). Characterization of the relationship of AAV capsid domain swapping to liver transduction efficiency. *Mol Ther*; **15:** 1955-1962.
29. Chen, SH, Habib, G, Yang, CY, u, ZW, Lee, BR, eng, SA, et al. (1987). Apolipoprotein B-48 is the product of a messenger RNA with an organ-specific in-frame stop codon. *Science*; **238:** 363-366.
30. Crooke, RM, Graham, MJ, Lemonidis, KM, Whipple, CP, Koo, S and Perera, RJ (2005). An apolipoprotein B antisense oligonucleotide lowers LDL cholesterol in hyperlipidemic mice without causing hepatic steatosis. *J Lipid Res*; **46:** 872-884.
31. Fazio, S and Linton, M (2001). Debate: "How low should LDL cholesterol be lowered?" Viewpoint: "It doesn't need to be very low". *Curr Control Trials in Cardiovasc Med*; **2:** 8-11.
32. Kastelein, JJP, Wedel, MK, Baker, BF, Su, J, Bradley, JD, Yu, RZ, et al. (2006). Potent reduction of apolipoprotein B and low-density lipoprotein cholesterol by short-term administration of an antisense inhibitor of apolipoprotein B. *Circulation*; **114:** 1729-1735.
33. Giering, JC, Grimm, D, Storm, TA and Kay, MA (2008). Expression of shRNA from a tissue-specific pol II promoter is an effective and safe RNAi therapeutic. *Mol Ther*; **16:** 1630-1636.
34. McBride, JL, Boudreau, RL, Harper, SQ, Staber, PD, Monteys, AM, Martins, I, et al. (2008). Artificial miRNAs mitigate shRNA-mediated toxicity in the brain: Implications for the therapeutic development of RNAi. *Proc Natl Acad Sci U S A*; **105:** 5868-5873.
35. Amendola, M, Passerini, L, Pucci, F, Gentner, B, Bacchetta, R and Naldini, L (2009). Regulated and multiple miRNA and siRNA delivery into primary cells by a lentiviral platform. *Mol Ther*; **17:** 1039-1052.
36. Schonfeld, G, Lin, X and Yue, P (2005). Familial hypobetalipoproteinemia: genetics and metabolism. *Cell Mol Life Sci*; **62:** 1372-1378.
37. Tarugi, P, Averna, M, Di Leo, E, Cefalu, AB, Noto, D, Magnolo, L, et al. (2007). Molecular diagnosis of hypobetalipoproteinemia: An ENID review. *Atherosclerosis*; **195:** e19-e27.
38. Straarup, EM, Fisker, N, Hedtjarn, M, Lindholm, MW, Rosenbohm, C, Aarup, V, et al. (2010). Short locked nucleic acid antisense oligonucleotides potently reduce apolipoprotein B mRNA and serum cholesterol in mice and non-human primates. *Nucl Acids Res*; **38:** 7100-7111.
39. Nishina, K, Unno, T, Uno, Y, Kubodera, T, Kanouchi, T, Mizusawa, H, et al. (2008). Efficient in vivo delivery of siRNA to the liver by conjugation of [alpha]-tocopherol. *Mol Ther*; **16:** 734-740.
40. Visser, ME, Akdim, F, Tribble, DL, Nederveen, AJ, Kwoh, TJ, Kastelein, JJP, et al. (2010). Effect of apolipoprotein-B synthesis inhibition on liver triglyceride content in patients with familial hypercholesterolemia. *J Lipid Res*; **51:** 1057-1062.
41. Kappel, S, Matthess, Y, Kaufmann, M and Strebhardt, K (2007). Silencing of mammalian genes by tetracycline-inducible shRNA expression. *Nat Protocols*; **2:** 3257-3269.
42. Doege, H, Grimm, D, Falcon, A, Tsang, B, Storm, TA, Xu, H, et al. (2008). Silencing of hepatic fatty acid transporter protein 5 in vivo reverses diet-induced non-alcoholic fatty liver disease and improves hyperglycemia. *J Biol Chem*; **283:** 22186-22192.
43. Zuker, M (2003). Mfold web server for nucleic acid folding and hybridization prediction. *Nucleic Acids Res*; **31:** 3406-3415.
44. McCarty, DM, Fu, H, Monahan, PE, Toulson, CE, Naik, P and Samulski, RJ (2003). Adeno-associated virus terminal repeat (TR) mutant generates self-complementary vectors to overcome the rate-limiting step to transduction in vivo. *Gene Ther*; **10:** 2112-2118.
45. Livak, KJ and Schmittgen, TD (2001). Analysis of relative gene expression data using real-time quantitative PCR and the 2-[delta][delta] CT method. *Methods*; **25:** 402-408.
46. Chen, C, Ridzon, DA, Broomer, AJ, Zhou, Z, Lee, DH, Nguyen, JT, et al. (2005). Real-time

quantification of microRNAs by stem-loop RT-PCR. *Nucl Acids Res*; **33:** e179.

47. Nathwani, AC, Gray, JT, Ng, CYC, Zhou, J, Spence, Y, Waddington, SN, et al. (2006). Self-complementary adeno-associated virus vectors containing a novel liver-specific human factor IX expression cassette enable highly efficient transduction of murine and nonhuman primate liver. *Blood*; **107:** 2653-2661.
48. Grimm, D, Pandey, K, Nakai, H, Storm, TA and Kay, MA (2006). Liver transduction with recombinant adeno-associated virus is primarily restricted by capsid serotype not vector genotype. *J Virol*; **80:** 426-439.
49. Gao, GP, Alvira, MR, Wang, L, Calcedo, R, Johnston, J and Wilson, JM (2002). Novel adeno-associated viruses from rhesus monkeys as vectors for human gene therapy. *Proc Natl Acad Sci U S A*; **99:** 11854-11859.
50. Zolotukhin, S, Byrne, BJ, Mason, E, Zolotukhin, I, Potter, M, Chesnut, K, et al. (1999). Recombinant adeno-associated virus purification using novel methods improves infectious titer and yield. *Nucleic Acids Res*; **6:** 973-985.